PAPER • **OPEN ACCESS**

Experimental investigation and numerical simulation of the thermosyphon heat pipe charged with R134a

To cite this article: S Y Zakaria *et al* 2020 *IOP Conf. Ser.: Mater. Sci. Eng.* **973** 012039

IOP Conf. Series: Materials Science and Engineering **973** (2020) 012039 doi:10.1088/1757-899X/973/1/012039

Experimental investigation and numerical simulation of the thermosyphon heat pipe charged with R134a

S Y Zakaria[1], A G Ibrahim[2], A M Rashad[3]and S E El-shamarka[4]
[1] MSc Researcher, Egyptian Armed Forces, Czakareya@yahoo.com.
[2]Assoc. Prof., MTC, Cairo,agmibrahim@hotmail.com.
[3]Assoc. Prof., MTC, Cairo, rashad@mtc.edu.eg.
[4]Prof.,Former Commandant of MTC, Cairo,selshamarka@mtc.edu.eg.
czakareya@yahoo.com

Abstract: This work presents an experimental and numerical study of Two-Phase Closed Thermosyphon (TPCT) heat pipe filledwith R134a as a base fluid. For this purpose, a test rig was designed and developed toperform a series of tests on the TPCT heat pipe by applying different heat inputs at the evaporator section. The surface temperature along the TCPT heat pipe and temperature changes of the cooling water across the condenser section were measured. The influence of the TCPT heat pipe operating conditions on its thermal performance was reviewed. The considered parameters were; heat pipe transport capacity, conductance, both heat transfer coefficients of the evaporator and condenser sections and the thermal efficiency. Then, a CFD model was developed to investigate the two-phase flow and heat transfer mechanism during the transient and steady-state operation of the TPCT heat pipe. The results of the experimental work were used to validate the CFD model and acceptable agreements were noticed. The validated CFD model is utilized to predict features of the mass and heat transfer processes, as well as the nucleate pool boiling and the liquid film condensation phenomena during TPCT heat pipe operation.

1. Introduction

Over the past decades, the applications of the thermosyphon heat pipe into thermal engineering systems are known, primarily in air conditioning systems, waste heat recovery, electronics cooling, chemical engineering, heat exchangers, water heater, solar collectors and power generation. The Two-Phase Closed Thermosyphon (TPCT) heat pipes have high effective coefficient thermal conductivity; Which can be significance orders greater than those of highly conductive solid materials, such as copper[1]. It consists of a tube or enclosed pipe consisting of a material, which is suitable with the working fluid, without wick structure lined on the inside pipe wall as shown in figure 1. It is partlycharged with a working fluid according to a specific filling ratio and then bolted; the mass of working fluid is selected, so that the heat pipe comprises both vapor and liquid through the operating temperature range. The degradation and failures of TPCT heat pipe thermal performance can occur in the sealed container wall, if any of the parts are not compatible (including the working fluid). The TPCT heat pipes are considered as passive heat transfer devices and constructed of three main sections:

- The evaporator section where the heat load is applied.
- The adiabatic section which is in the middle of the TPCT heat pipe.
- The condenser section where the heat load is rejected.

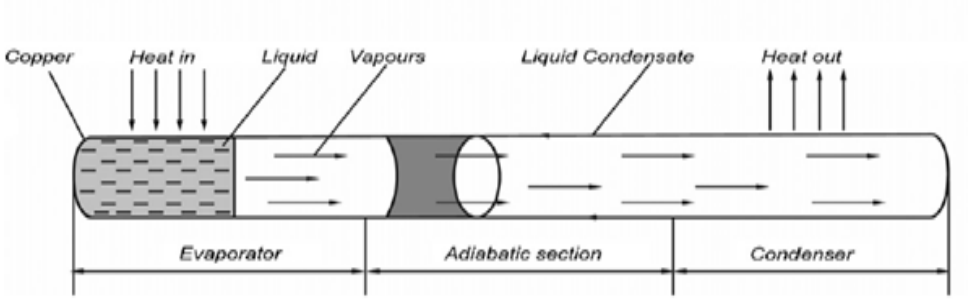

Figure 1. The construction for a TPCT heat pipe, [2].

The main advantages of TPCT heat pipe are low manufacturing cost, high heat fluxes transport and simple construction rather than the other heat pipes. For low temperature applications, different refrigerants like R404, R134a, R22, R410a and ammonia which are selected as working fluids with compatible metals of sealed shell as steel, aluminum and copper are used. For medium temperature applications, water is considered a compatible working fluid for temperatures from30 °Cto300 °C, with good compatibility with different metals counting stainless steel and copper. For high temperature applications, different organic fluids and liquid metals are selected as working fluids for operating temperature above 300 °C. As heat pipe principle of work depends on the working fluid phase change to transfer heat from heat source to heat sink or heat distribution, working fluid charged in heat pipe which has an important role to consolidate the heat pipe thermal performance[3]&[4]. Concerning the importance of TPCT heat pipe applications, several researches have been carried out to investigateits thermal performance with severaldesign parameters, base fluids, materials, geometries, filling ratios and different operating conditions, heat load, inclination, etc. .

Naphon et al.[5]presented an experimental study by using a fabricated heat pipe with 600 mm length and 15 mm diameter from straight copper tube. The heat pipe is tested with alcohol, de-ionic water and alcohol-titanium nanofluids. The reported work indicated the influence of heat pipe tilt angle, filling ratio of working fluid and concentrations of nanoparticles volume on the performance of heat pipe.Results showed that an enhancement in thethermal efficiency of heat pipe with utilizing nanofluids as working fluids compared to use of based fluids.

Tsai et al. [6]compared the common steady-states test with a novel dynamic test method to investigate; shapes of heat pipes, filling ratios and bending angle showing their effect on performance. Experimental results indicated that the heat pipe performance would deteriorate considerably due to deformation of heat pipes. The operation limitations were increased due to larger filling ratios.

Attia and El-Assal[7]presented experimental study on heat pipe filled with methyl alcohol and water to examine heat pipe thermal performance at different filling ratios, and solution of propylene glycol and water were tested to investigate the influence of using surfactant at two concentrations.The results showed that using water as working fluid indicates much better thermal performance than using methyl alcohol. The filling ratio 30% was optimum for most tested working fluids. Using surfactant with water was much better than using pure water.

Wang et al. [8]presented an experimental work to examine an inclined miniature mesh heat pipe charged with water-CuOnanofluid as working fluid. The aim of this workwas to show the effects of operating temperature and the inclination angle on heat pipe performance. Results showed a considerableinfluence on heat pipe thermal performance charged with water-CuOnanofluiddue to inclination angle.The best results were obtained at 45° inclination angle of heat pipe.

Peyghambarzadeh et al [9]reported an experimental work to study a multi-evaporator heat pipe charged with three working fluids (methanol, water and ethanol). Low heat flux inputs are applied at evaporator section (up to 2500 W/m^2), a water coolant is circulating at constant temperature across condenser section with three levels 15, 25 and 35 °C. Experimental results showedthat evaporator heat transfer coefficient was increased with increasing heat flux input. It was noticed for methanol at high heat flux input, the heat transfer coefficient was degraded due to dryout effect at evaporator section.

An improvement in heat transfer coefficients were acquired for ethanol and water compared to methanol anddegradationin the thermal resistance of heat pipe with increasing the inclination angle.

Aniket and Ravindra[10]focused on operating parameters effect on TPCT heat pipe performance parameters such as heat load, coolant mass flow rate, aspect ratio, inclination angle and filling ratio. The novel heat transfer techniques were illustrated such as CFD modeling and analysis, resurfacing and use of ultrasonic wave. This study indicated the need of mathematical modeling of thermosyphon thermal operation with new efficient and minimum global worming potential refrigerants.

Fadhl et al. [11]presented a numerical simulation model of a thermosyphon heat pipe charged with water as base fluid using the volume of fluid (VOF) method in FLUENT ANSYS. Thismodel simulated the two-phaseflow, mass and heat transfer processes over heat pipe operation. The numerical model wasverified using experimental data at the same condition, and a good agreement was observed.

Abou-Ziyan et al [12]Noticed during their studies that the adiabatic mean temperature is very similar to the saturation temperature ofworking fluid. EL-Genk and Huang [13]reportedthe saturation temperature at the end of adiabatic section. Those results were utilized for computation the evaporator and condenser heattransfercoefficients.

Noie[14]investigated experimentally a vertical copperTPCT heat pipe on steady-state condition of total length 980 mm, outside diameter 32 mm and thickness 3.5 mm charged with distilled water. According to input heat rates from 100 to 900 W, filling ratio from 0.3 to 0.9, and the evaporator lengths for aspect ratios7.45, 9.8, and 11.8. The wall surface temperature of the TPCT heat pipe, the applied heat to evaporatorsection and rejected heat from condenser section were defined, also. A comparison of experimental evaporation heat transfer coefficient with current correlations was presented. The results showed the optimum filling ratio for a specific aspect ratio, that the TPCT heat pipe is operating at its best.

Wang et al.[15]performed a CFD model to stimulate the geyser boiling conception in a TPCT heat pipe. The commonly used Lee modelis enhanced by presenting the regard of superheat to raise the predicted performance. CFD simulation of heat transfer process was achieved using both original and enhanced Lee model using VOF technique.These results were evaluated and compared to those from experiments. From experimental results, the cycle time of 80-100s is occurred at 400 mL/min at (95°C) flow rate of heating water and 300 mL/min at (30°C) of cooling water. The conformable modeling resulted in agreement with the experimental data at same conditions proposed that the enhanced Lee model has a better expectation performance.

Alizadehdakhelet al.[16]carried out a numerical model using VOF method to investigate the vapor/liquid two phases interaction. Experiments were performed at severalworking conditions. The predicted wall temperatures gradient from the numerical model showed a good agreement with those from experimental tests results. This concluded that the usage of CFD as a proposed technique to simulate and clarify the two-phase flow and heat transfer process in heat pipes.

Asmaie et al.[17]performed CFD model of TPCT heat pipe filled with two base fluids deionized water and CuO/Water nanofluid. The results showed that, the ability of thermosyphon to transport heat load is increased about 46 % higher with usage of nanofluid as operating fluid than that of water, Moreover the volume concentration of 1 wt. % was found as the best concentration, and a reduction in thermosyphon heat pipe wall temperature was observed with increasing the nanofluid concentration in base fluid.

As yet, there isneeding of new studies and researches to explain the heat transfer features of TPCTheat pipe to improve its thermal performance in different thermal engineering applications. This study investigates, experimentally and numerically, the thermal performance of a TPCT heat pipe. Different performance parameters, which have a substantial effect on application of TPCT heat pipe in engineering systems, namely; heat transport capacity, heattransfer coefficients, thermal conductance and overall thermal efficiency are reported under different heat loads.

This article is organized as follows. The of heat pipe performance indices are summarized in the next section, the general design of the experimental test stand and experimental results are described. Then, the development of numerical model and validation of simulation results are presented. Finally, the main findings of present work conclude the paper.

2. Performance parameters

The considered parameters utilized to estimate the thermal performance of the TPCT heat pipe are summarized as follows:

2.1. Heat transport capacity

The heat transport capacitywas specified by determining the mass flow rate, temperature changes of coolant water through the condenser section.

$$\dot{Q}_{out} = \dot{m}\, C\, (T_{out} - T_{in}) \quad (1)$$

2.2. Heat transfer coefficients

At the evaporatorsection, from experimental measurements theevaporatorheattransfer coefficient is definedby the equation:

$$h_{ev} = \frac{\dot{Q}_{in}}{A_{ev}\ (T_{ev} - \widetilde{T_{ad}})} \quad (2)$$

At the condenser section, from experimental measurements the condenser heat transfer coefficient is defined by the equation:

$$h_{con} = \frac{\dot{Q}_{in}}{A_{con}\ (\widetilde{T_{ad}} - T_{con})} \quad (3)$$

2.3. Thermal conductance

The thermal conductance represents the ability of thermosyphon to transport input heat. It is computed using the equation:

$$c = \frac{\dot{Q}_{in}}{(T_{ev} - T_{con})} \quad (4)$$

2.4. The overall thermal efficiency

The overall thermosyphon thermal efficiency is computed using the equation:

$$\eta_{th} = \frac{\dot{Q}_{out}}{\dot{Q}_{in}} \quad (5)$$

3. Experimental work

3.1. Experimental set-up

The experimental system was built to measure the surface temperature profiles of the TPCT heat pipeat variable operating conditions. Figure 2presentsthe scheme of the experimental arrangement forthetested TPCT heat pipe in vertical position. The tested TPCT heat pipe is made from standard red copper tube. The tube has 1400 mm total length, 20 mminner diameter and 1 mm wall thickness. The investigated heat pipe is filled with R134a. Closure of the heat pipe is made by soldering brass cap at both ends. The TPCT heat pipe is consisted of three main sections; evaporator, adiabatic and condenser sections. The specifications of the tested thermosyphon are listed in table 1.

The evaporator section is located in lower end of the pipe; the thermal power is supplied by mean of a wire heater of Nickel – Chrome. The electrical resistance (3.334 ohm/m) is uniformly coiled the evaporator section surface such that to guarantee it is not close to thermocouples. The input electric power to electric tape is measured in each experiment and adjusted via a Variac resistance. The thermosyphon evaporator section is insulated by a high-density wool glass isolator to minimize heat losses during experiments. The evaporator section cap end is insulated. The temperature at the surface of wool glass isolator is measured to determine the heat losses by natural convection at the

evaporator section. The evaporator wall surface temperature is measured by means of three calibrated (NiCr - Ni) K – type thermocouples. The thermocouples are embedded on the evaporator outside wall surface and spaced on specific locations on the evaporator circumference along its length.

Similarly, the adiabatic section in-between evaporator and condenser sections is insulated by high density wool glass insulator and its wall temperature surface is measured by two spaced calibrated (NiCr - Ni) K - type thermocouples.

In the top end of the pipe the condenser section is located. A glass cooling water jacket of length 350 mm, 40 mm inside diameter and 2 mm thickness insulated by high density wool glass is mounted around the condenser section overall length as the cooling of condenser is accomplished by circulating water through the glass jacket. The temperatures of water inlet and outlet are measured by two calibrated (NiCr - Ni) K - type thermocouples. The water mass flow is adjusted and measured at each experiment. To ensure steady flow rate of water to the condenser cooling water jacket during experiments, an overhead tank is used. Also, the condenser wall surface temperature is measured by three spaced calibrated (NiCr - Ni) K - type thermocouples.

All the reading measurements of the eight thermocouples that are embedded on the outside wall surface of three sections of the thermosyphon are logged by lab view program through two analog data acquisition cards for thermocouples. Figure 3shows the main components of the tested thermosyphon, while figure 4shows the locations of thermocouples along the thermosyphon.

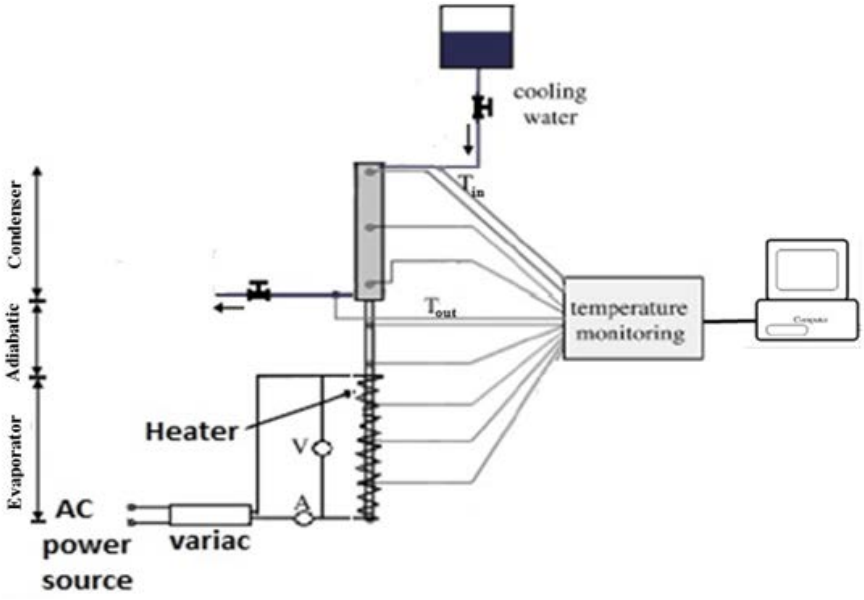

Figure 2. A scheme of the experimental arrangement.

Table 1. The specifications of the tested thermosyphon.

Material	Red copper
Total length	1400 mm
Evaporator length	550 mm
Adiabatic length	500 mm
Condenser length	350 mm
Outside diameter	22 mm
Wall thickness	1 mm
Filling ratio	100%
Working fluid	R134a
Working fluid temperature range	- 40:100 °C

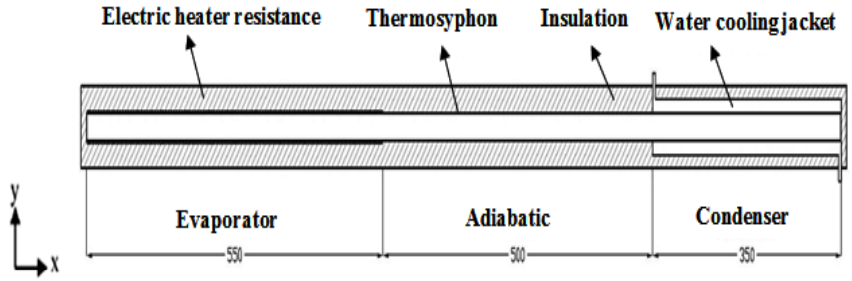

Figure 3. A longitudinal cross section of thermosyphon heat pip.

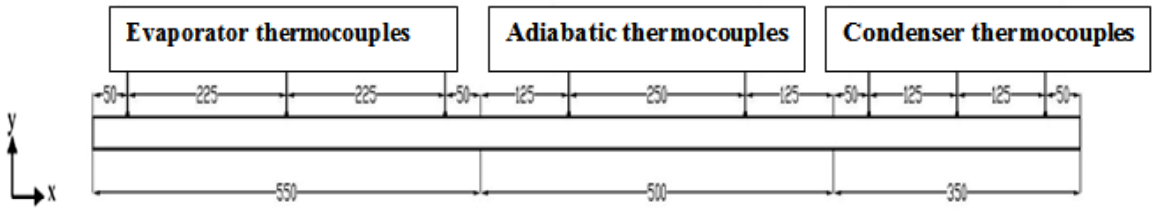

Figure 4. Locations of thermocouples along the thermosyphon heat pipe.

3.2. Test procedure

The water flow rate was adjusted to the required value at the beginning of each steady-state test, and then the electrical heat load was set to the evaporatorsection. A constant working pressure was achieved by balancing the rate of heat load added to the evaporator section to heat rejected from the condenser section. After that, the equipment waspermitted to stabilize about 20 min before recording any readings. By using the two analog data acquisition cards,all temperatures from the thermocouples were registered. As soon as, a steady state was established within (15 - 20) min, thermocouples temperature and power readings were recorded. For different power inputs from 30.4 to125.4 W, the process was repeated. This range was investigated in order to ensure reliableperformance of the TPCT heat pipe within a prolonged workingperiod. To ensure that there was no degradation of the TPCT heat pipeperformance was occurredalong operation, the 2-h observing period was considered.

3.3. Experimental results

The experimental study of the performance characteristics for a TPCT heat pipe, according to different heat loads to evaporator section, includes; thermosyphon transient response, output heat at condenser section, surface temperature profilethroughout the thermosyphon, heat transfer coefficient at both evaporator and condenser sections,conductance of thermosyphon and overall thermal efficiency. The experimental results are presented in next sections.

3.3.1 Heat transport capacity. The experimental technique is imitated by adjustment of the cooling water flow rate across the condenser section, to accomplish a reasonable temperature variation across it during whole test period using overhead tank, then applying the desired input power to the warred electric heater along evaporator surface. The applied heat load to evaporator section is increasedsteadily, to begin a new test. All test parameters are evaluated and registered once the steady-state is established. Figure 5shows output heat from condenser section as a function of applied input heat to evaporator section.The output heat rises with increasing input heat.

3.3.2 Surface temperature. The surface temperatures at the different sections of TPCT heat pipe are shown in figure 6 for different heat loads from 30.4 to 125.4 W. The temperature over the outer surface of the TPCT heat pipe was recorded at eight different locations.The surface temperature

profile according to each constant input heat load is obtained at the steady state condition and it was recorded for 2 h to grantee the stabilization thermal operating cycle of the heat pipe.
As depicted from figure 6the surface temperature in the thermosyphon sections is almost uniform; the difference in temperature is within (3-10) °C.

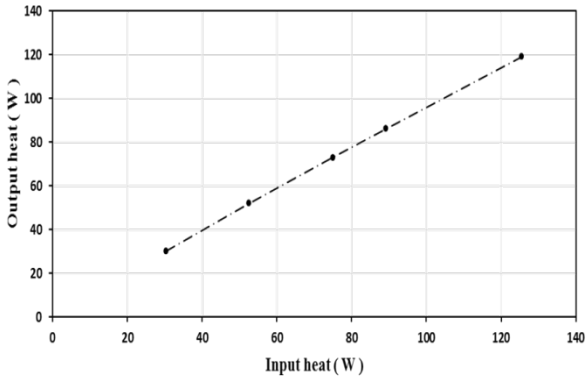

Figure 5. Heat transport capacity according different heat inputs.

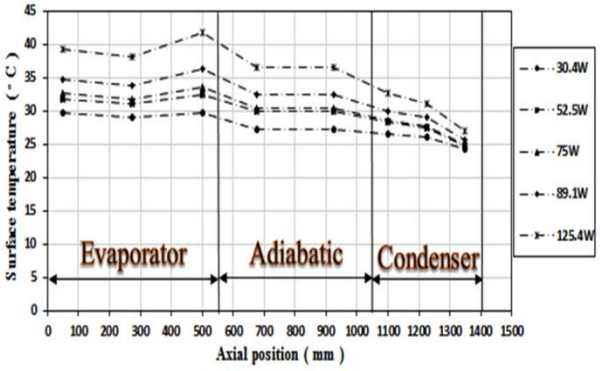

Figure 6. Surface temperature profiles along the thermosyphon.

3.3.3 Heat transfer coefficients. Figure7 and figure 8show the evaporator and condenser sections heat transfer coefficients respectively against the input-heat at evaporator section. As shown in these figures, at constant working pressure, the heat transfer coefficients of the evaporator and condenser increase by increasing the input heat into the evaporator section.

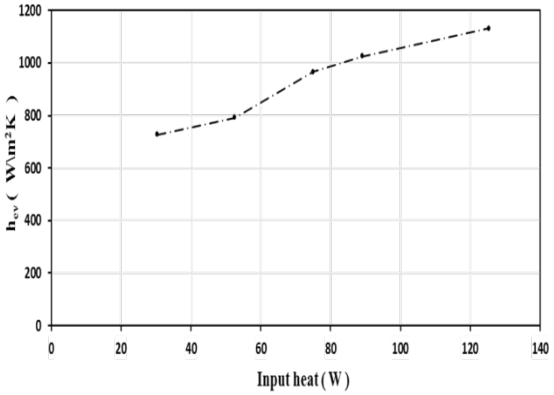

Figure 7. Evaporator heat transfer coefficient according to several heats input.

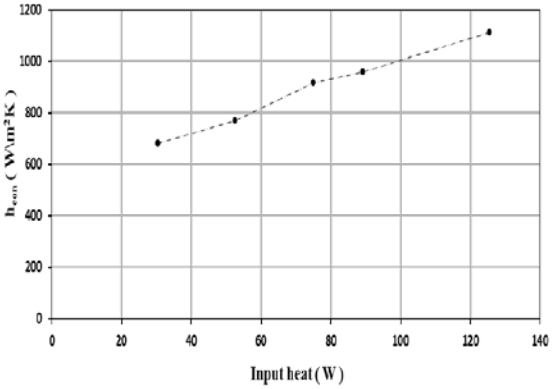

Figure 8. Condenser heat transfer coefficient according to several heats input.

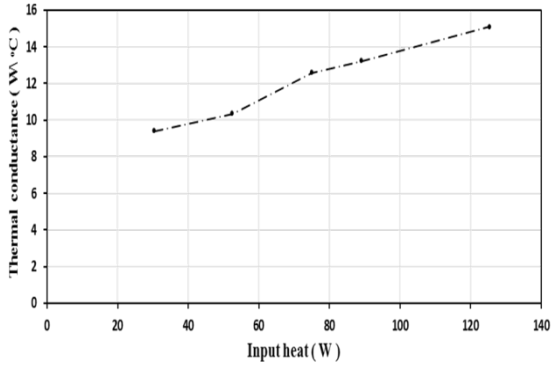

Figure 9. Thermal conductance variation according to different heat inputs.

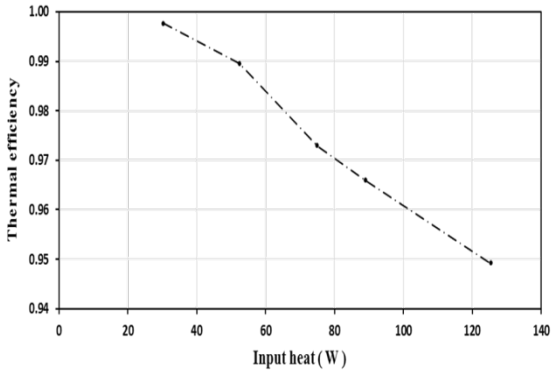

Figure 10. Thermal efficiency variation according to different heat inputs.

3.3.4 Thermal conductance. Figure 9 shows the thermosyphon thermal conductance variation with different heat inputs at evaporator section. It increases with increasing input heat at evaporator section, showing the ability of thermosyphon to transport input heat.

3.3.5 Thermal efficiency. Figure 10 shows the overall thermosyphon thermal efficiency according to differentheatinputs at evaporator section. It was shown that thermosyphon thermal efficiency decreases with increase input heat at evaporatorsection.

4. Numerical simulation

In the current work, the numerical simulation of TPCT heat pipe is performed by CFD approach. The commercial package ANSYS FLUENT 18.1 [18] and the VOF method were applied for the modeling of TPCT heat pipe. Throughout the functioning of TPCT heat pipe,the phase changes continuously from liquid to vapor phase and vice versa due to pool boiling inside the evaporator section and film condensation inside the condenser section, respectively. The VOF method defines the volume fraction in the cells of the simulated domain for each phase (liquid / vapor). To simulate phase change processes, customized mass and energy source terms to the offeredNavier-Stokes equations in the ANSYS FLUENT 18.1 kit were employed.

For the evaporation process, to compute mass quantity released from the liquid phase and the mass quantity additional to the vapor phase, two mass source terms were used. Similarly for the condensation process, two mass sources specifying the vapor mass transferquantity to the liquid phase were applied.

For heat flow, only one source term for two phases was employed in the evaporation or condensation processes. The heat transfer was defined by multiplying one mass source term by the latent heat of evaporation. Additionally, instead of liquid or vapor temperature a mixture temperature was presented, because of the VOF method combines parameters such as temperature and velocity with the mixture phase, not with a specified one.

4.1. Computational domain

In order to simulate two phase heat transfer process in tested TPCT heat pipe, a two-dimensional model was produced. The total length 1400 mm, 22 mm andwall thickness 1 mm of closed copper tube were applied to the model geometry. The lengths of the evaporator, adiabatic and condenser sections were represented as 550,500 and 350 mm, respectively.

4.2. Mesh generation

The two-dimensional geometry is meshed using GAMBIT's grid generation software. The evaporator section contains 26,400 cells, the adiabatic section contains 24,000 cells and the condenser section contains 16,800 cells. As a result, 67,200 Quad cells are generated for liquid regions. Nearby to the TPCT heat pipe inner walls, fifteen layers of cells wereutilized to take the thin liquid film that obtains near the walls. The size of first grid was 0.01 mm with growth ratio 1.2, as shown in figure 11.

Various mesh sizes were applied to test grid independence as shown in figure 12. The mean surface temperatures of the evaporator ($\widetilde{T_{ev}}$), adiabatic ($\widetilde{T_{ad}}$) and condenser ($\widetilde{T_{con}}$) sections for various sizes of mesh were compared and shown in 'Table 2' for input heat load 30.4 W. It was observed that nearly the similarmean surface temperature differences at different sections were acquired for various mesh sizes. Hence, the mesh size of 67,200 Quad, Map cells is chosen for the modeling study.

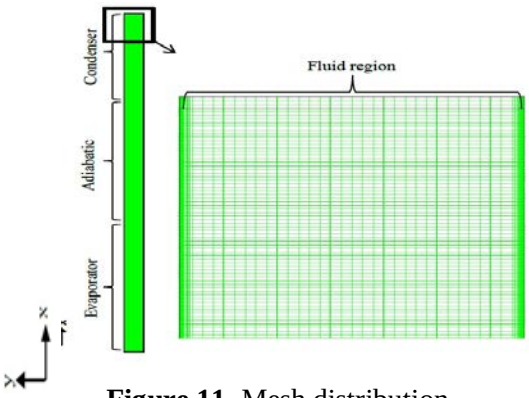

Figure 11. Mesh distribution.

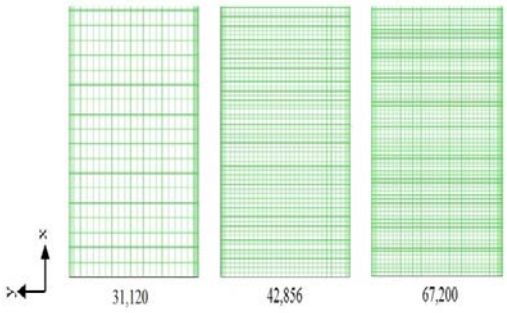

Figure 12. A section of the computational meshes.

Table 2. Grid independence results for the TPCT heat pipe charged with R134a for heat input of 30.4 W.

Mesh size	31,120	42,856	67,200
$\widetilde{T_{ev}}$ °C	29.85	29.75	29.77
$\widetilde{T_{ad}}$ °C	25.22	25.22	25.22
$\widetilde{T_{con}}$ °C	24.02	24.02	24.02

4.3.Boundary conditions

A constant heat flux at the evaporator wall, a zero-heat flux at adiabatic wall, the upper and lower caps of the TPCT heat pipe assuming these regions are insulated and a convection heat transfer coefficient at condenser wall, were defined as boundary conditions.Ano-slip boundary condition is defined at the inner walls of the TPCT heat pipe.It is consideredthat the filling ratio 100%, i.e.FR = 1.0, for R134a charged the TPCT heat pipe. By using the mesh adaption ability in ANSYS FLUENT 18.1wasutilizedto describethe filling ratio at the evaporator section.

Referring to experimental results, the temperature variation along evaporator and condenser sections was restricted to 10 deg. Hence, the thermo-physical property of R134a is supposed to be temperature-independent to decrease thecomputationaltime.These properties are shown in 'Table 3'. The density of the liquid phase (ρ_l) is defined as:

$$\rho_l(\mathrm{T}) = \sum_{i=0}^{n=4} \mathrm{C_i} \cdot \mathrm{T^i} \quad (6)$$

The influence of surface tension (σ_{lv}) over the interface between the liquid-vapor phases is comprised in the model by applying the following correlation:

$$\sigma_{lv}(T) = \sum_{i=0}^{n=3} \mathrm{B_i} \cdot \mathrm{T^i} \quad (7)$$

Where C_i and B_i are shown in table 4.

Table 3. Thermo-physical properties of R134a, [19].

Physical property	Value	Unit
Latent heat of evaporation	177.79	kJ/kg
Density of vapor phase	32.35	kg/m^3
Specific heat of liquid phase	1.4246	kJ/kg.K
Specific heat of vapor phase	1.0316	kJ/kg.K
Thermal conductivity of liquid phase	0.081134	W/m.K
Thermal conductivity of vapor phase	0.013825	W/m.K
Viscosity of liquid phase	$1.9489x10^{-04}$	kg/m.s
Viscosity of vapor phase	$1.1693x10^{-05}$	kg/m.s
Molecular weight	102.03	kg/kmol
Critical temperature	374.21	K
Critical pressure	40593	kPa

Table 4. Density and surface tension correlations for R134a, [19].

	Density (ρ_l)			
C_0	**C_1**	**C_2**	**C_3**	**C_4**
3952.801	- 25.9914	0.09482	-1.290×10^{-04}	0
	Surface tension (σ_{lv})			
B_0	**B_1**	**B_2**	**B_3**	**-**
0.04929	-8.34×10^{-05}	-3.95×10^{-07}	7.071×10^{-10}	-

4.4. Solution procedure and convergence criterion

With a time step 0.001 s,a transient simulation is performed to model the dynamic behavior of the liquid-vapor flow and the evaporation and the condensation processes. This time step was designated according to the courant number, representing the ratio of the time step to the fluid time fluid needs to move through a cell. In this CFD model, the interaction between two phases was detected by solving the continuity equation to determine each phase volume fraction, and the energy equation was solved to observe the temperature through the computational domain. The flow is assumed to be laminar. FLUENT offers several algorithms for pressure-velocity coupling. The SIMPLE algorithm for pressure-velocity coupling and a first-order upwind scheme for the definition of momentum and energy were chosen in the model.

When the scaling residuals are $10^{-5}$for volume fraction and velocity components and $10^{-6}$for temperature variable, the numerical calculation is converged. Through the CFD computational domain the governing equations are solved such that variables of the governing equations are defined by the entity of the particular phase in each cell in the computational domain. The primary and secondary phases are described as vapor and liquid phases, respectively. In the material properties format the saturation temperature and the latent heat of evaporation are defined.

4.5. CFD simulation results

4.5.1 Heat transfer process. The operating conditions were set to saturation values (25 °C)at the start of heating process. At the evaporator section a constant heat flux is defined, evaporating heat transfer keeps on the wall of the evaporator section. The generated vapor moves across the adiabatic section to reach the condenser section due to that a high temperature region shows in the condenser section. The region near the condenser interior wall has a lower temperature than the central region that causes vapor condensing over the interior wall of the condenser section. After 287 s the steady state is achieved as the temperature appearedintothe TPCT heat pipeseems uniform, figure 13shows temperature distribution contour inside TPCT heat pipe.

4.5.2 Evaporation process. During the evaporation the pool boiling process occurs within the evaporator section was visualized. Figure 14illustrates the volume fraction contour distribution within the evaporator section,the blue color represents liquid phase with value 0 of the vapor volume fraction and the red color represents the vapor phase with value 1of the vapor volume fraction.

A localized natural convection flows can be seen at the lower half of the evaporator regionbecause of a minor rise of the working fluid saturation pressure / temperature. The adjacent liquid film to the wall starts to boil, the neighboring liquid film to the wall begins to boil therefore essential radii are surpassed at the local nucleation places so that persistent nucleation takes place. Vapor bubbles begin to form at these places where the liquid boils. Then, the isolated vapor bubbles develop and float to the top of the liquid pool before decomposition and release of their vapor quantity. Through this cycle, the volume fraction of the liquid phase reduces while the volume fraction of the vapor phase increases in the region of the evaporator.

4.5.3 Condensation process. Following to the liquid pool boiling process, the saturated vapor movesacross the adiabatic regionreaches the condenser region. As the saturated vapor contacts the

condenser's surface, the vapor condenses over the inner cold wall of the condenser region developing a liquid film. Figure 14 illustrates the condensate film configuration.
Under gravity effect this liquid film will drop down across the adiabatic region, the liquid pool in the evaporator region will be filled by a continued thin liquid film. During the above cycle, the latent heat of evaporation that was stored in the evaporator region is extracted by the vapor and released due to phase change process occurred at the inner wall of the condenser region.

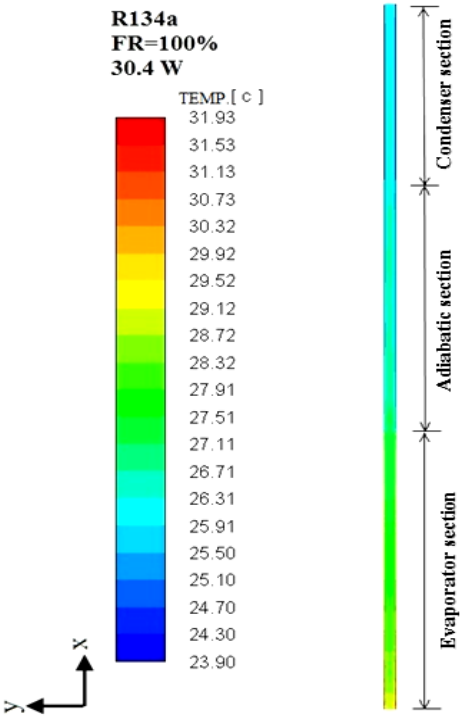

Figure 13. Temperature distribution contour for R134a filled thermosyphon at steady state.

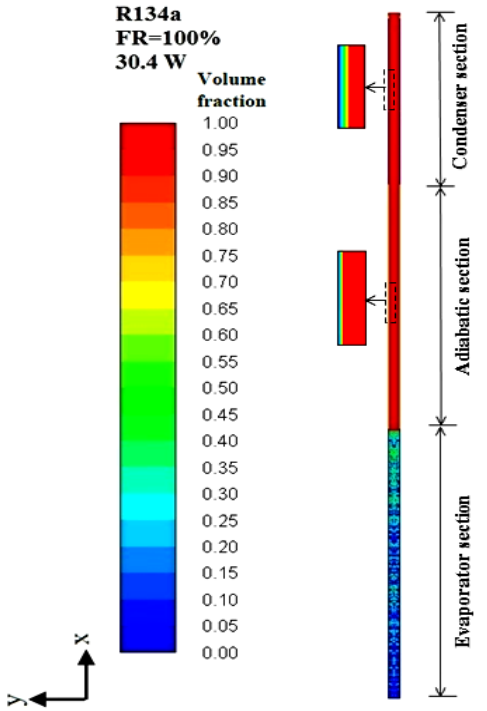

Figure 14. Volume fraction contour for R134a filled thermosyphon at steady state.

5. Validation of CFD simulation results

Figure 15shows the experimental and CFD simulation temperature distribution profiles over the R134a charged the TPCT heat pipe, for applied heat load 30.4 W. As depicted in figure 15 the simulation results presentedan acceptable agreement with the experimental data. The simulation results of temperature profile werereviewed with the experimental data by defining the average relative error (*ARE*). As a result of this,*ARE*of the evaporator, adiabatic and condenser average wall temperatures are 1.01 %, 7.51 % and 6.08 %, separately, table 5.

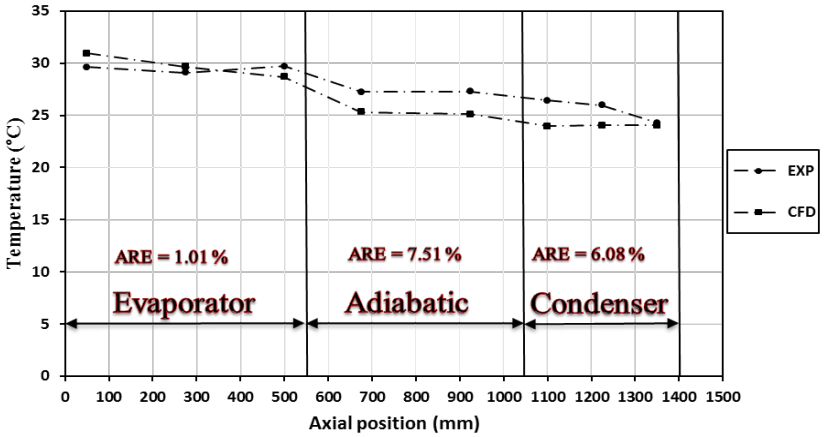

Figure 15. Temperature distribution profiles for experiment and CFD simulation.

Table 5. Comparison between experimental data and CFD simulation for heat input 30.4 W.

Section	Position	T_{EXP}	T_{CFD}	$\Delta T_{EXP-CFD}$	RE	$\widetilde{T_{EXP}}$	$\widetilde{T_{CFD}}$	$\Delta\widetilde{T_{EXP-CFD}}$	ARE
		°C	°C	°C	%	°C	°C	°C	%
Evaporator	T_{e1}	29.62	30.93	1.31	4.43	29.48	29.77	0.3	1.01
	T_{e2}	29.11	29.69	0.58	2.00				
	T_{e3}	29.70	28.70	1.00	3.36				
Adiabatic	T_{a1}	27.25	25.33	1.92	7.05	27.27	25.22	2.05	7.51
	T_{a2}	27.29	25.11	2.18	7.97				
Condenser	T_{c1}	26.43	23.97	2.46	9.32	25.57	24.02	1.55	6.08
	T_{c2}	25.99	24.04	1.95	7.50				
	T_{c3}	24.30	24.05	0.25	1.02				

6. Conclusions

The present study reports a numerical simulation of TPCT heat pipe filled with R134a. The advanced CFD model considered the nucleate pool boiling and the liquid film condensationprocesses occurred during operation of the TPCT heat pipe. The CFD model results are validated with the experimental data at the same working conditions. The comparison between experimental and numerical results indicated the good ability of the CFD model. The capabilities of validated CFD model will be used to derive the limitations that can restrict the transportation of heat pipe fluid in satellite application.

References

[1] Chang YW, Cheng CH, Wang JC and Chen SL 2008 *Energy Conv. and Mgmt.***49**3398-404
[2] Huminic G, Huminic A, Morjan I and Dumitrache F 2011, *Int. J. of Heat and Mass Transfer***54**656-61
[3] Liu ZH and Li YY. 2012*Int. J. of Heat and Mass Transfer***55**6786-97
[4] Liu ZH, Li YY and Bao R 2011*Int. J. of Thermal Sciences***50**558-68
[5] NaphonP, AssadamongkolP and BorirakT 2008*Int. Comm. in Heat and Mass Transfer***35**1316-19
[6] Tsai TE, Wu GW, Chang CC, Shih WP and Chen SL 2010 *Int. J. of Heat and Mass Transfer***53**4567-78
[7] Attia A A and El-Assal B T 2012*Heat Pipe Science and Technology, An Int. J.***3**35-51
[8] Wang PY, Chen XJ, Liu ZH and Liu YP 2012 *Thermochimica Acta***539**100-08
[9] PeyghambarzadehS, Shahpouri S, Aslanzadeh N and Rahimnejad M 2013 *Ain Shams Engineering J.***4**855-61
[10] AniketD P and Ravindra B Y 2012 *Int. J. of Emerging Technology and Advanced Engineering***2**202-06

[11] Fadhl B, Wrobel L C and Jouhara H 2013 *App. Therm. Eng.***60**122-31
[12] Abou-ZiyanH, Helali A, Fatouh M and El-Nasr M A 2001 *App.Therm.Eng.***21**813-30
[13] El-GenkM Sand Lianmin H 1993 *Int. J. of Heat and Mass Transfer***36**3823-30
[14] Noie S 2005*App. Therm. Eng.***25**495-506
[15] Wang X, Wang Y, Chen H, and Zhu Y 2018 *Int. J. of Heat and Mass Transfer***121**703-14.
[16] Alizadehdakhel A, Rahimi M and Alsairafi A A 2010 *Int. Comm. in Heat and Mass Transfer***37**312-18
[17] Asmaie L, Haghshenasfard M, Mehrabani-Zeinabad A and Esfahany M N 2013 *Heat and Mass Transfer***49**667-78
[18] Ansys FLUENT Theory Guide *2017* (Release 18.0).*Multiphase Flows. ANSYS, Inc.* 715-46
[19] Lemmon E, Huber M and McLinden M 2010 *NIST Standard Reference Database 23, Reference Fluid Thermodynamic and Transport Properties (REFPROP)* ver 9.0 National Institute of Standards and Technology.

N**omenclature**

A	Area (m^2)
C	Water specific heat (J/kg.°C)
c	Conductance (W/ °C)
h	Heat transfer coefficient (W/m^2.°C)
$\dot{Q}$	Heat rate (W)
T	Temperature (°C)
$\dot{m}$	Mass flow rate (kg/sec)

Greek symbols

η_{th}	Thermal efficiency
α	Volume fraction
ρ	Density (kg/m^3)
σ	Surface tension coefficient (N/m)

Superscripts

˜	Average

Subscripts

ev	Evaporator
ad	Adiabatic
con	Condenser
in	Inlet
out	Outlet
l	Liquid phase
v	Vapor phase